Universality of Returning Electron Wave Packet in High-Order Harmonic Generation with Midinfrared Laser Pulses

Anh-Thu Le,[1] Hui Wei,[1] Cheng Jin,[1] Vu Ngoc Tuoc,[2] Toru Morishita,[3] and C. D. Lin[1]

[1]*Department of Physics, Cardwell Hall, Kansas State University, Manhattan, Kansas 66506, USA*
[2]*Institute of Engineering Physics, Hanoi University of Science and Technology, 1 Dai Co Viet Road, Hanoi 10000, Vietnam*
[3]*Department of Engineering Science, University of Electro-Communications, 1-5-1 Chofu-ga-oka, Chofu-shi, Tokyo 182-8585, Japan*

We show that a returning electron wave packet in high-order harmonic generation (HHG) with midinfrared laser pulses converges to a universal limit for a laser wavelength above about 3 μm. The results are consistent among the different methods: a numerical solution of the time-dependent Schrödinger equation, the strong-field approximation, and the quantum orbits theory. We further analyze how the contribution from different electron "trajectories" survives the macroscopic propagation in the medium. Our result thus provides a new framework for investigating the wavelength scaling law for the HHG yields.

High-order harmonic generation (HHG) has been a very active field of research over the last two decades. With the popular Ti:sapphire laser operating at an 800-nm wavelength, a great deal of experimental and theoretical research has been carried out. This interest is due to two facts. First, HHG provides a tabletop coherent extreme ultraviolet (XUV) light source [1] that can be used for application in science and technology. In particular, it can serve as a source of attosecond pulses [2,3] and attosecond-pulse train [4]. Second, the HHG signal contains information about the target structure [5–7]. As few-cycle laser pulses are routinely available, HHG holds great promise to become a spectroscopic tool capable of providing a femtosecond scale temporal resolution.

The typical photon energy range available from HHG sources with a Ti:sapphire laser has been limited to about 100 eV or so. The well-known cutoff law $\Omega_c = I_p + 3.17U_p$, with Ω_c, I_p, and $U_p \propto I_0\lambda^2$ being the cutoff energy, the ionization potential of the target, and the ponderomotive energy, respectively, suggests that higher energy photons can be produced with longer driving laser wavelengths λ (atomic units are used throughout, unless otherwise indicated). Increasing the peak laser intensity I_0 is not an option because of the ground-state depletion as well as the phase mismatch caused by excessive free electrons in the medium. With recent development in optical parametric amplification techniques, midinfrared (mid-IR) lasers with a wavelength of a few microns are available today, with a sufficient intensity to generate high harmonics, thus pushing the HHG photon energy range beyond the water window and even to the keV region [8–11].

Wavelength scaling of HHG yield has been studied both theoretically [12–19] and experimentally [20,21]. Early theoretical investigation was mostly based on numerical solution of the time-dependent Schrödinger equation (TDSE) [12–14]. These studies showed that, apart from small oscillation on a fine λ scale due to the threshold phenomena effect, harmonic yield at constant driving laser intensity drops drastically as λ^{-x}, with $x \approx$ 5–6. All these studies have been limited to wavelengths below 2 μm, and the analysis mostly for a fixed energy range from 20 to 50 eV. More recent studies within the strong-field approximation (SFA) [16–18,22] showed scaling behavior with somewhat slightly different x. By using the quantum orbits (QO) theory [23–25], scaling law for long and short trajectories have also been reported [18,19].

At constant laser intensity, Keldysh parameter $\gamma = \sqrt{I_p/(2U_p)}$ scales as $1/\lambda$. It is therefore expected that longer wavelengths would drive the interaction further into the tunneling regime ($\gamma \ll 1$), where the semiclassical description (as in the SFA) would be more accurate. For subtleties related to the Keldysh parameter we refer the reader to the recent discussion by Reiss [26] as well as within the framework of the recently developed adiabatic theory [27] for the range of applicability.

According to the quantitative rescattering model [7,28–31], HHG yield is a product of the returning electron wave packet and the photorecombination cross section. The latter is target dependent and varies strongly with energy. As a consequence, the scaling law for HHG yield is not only target specific, but also depends on the HHG photon energy, as evident in Refs. [13,14,31]. The goal of this Letter is to explore the scaling law for the returning electron wave packet. This approach allows us to identify a universal shape of the wave packet as a function of a scaled energy in the long wavelength limit. The universal shape is nearly identical for all atomic targets we considered, including atomic hydrogen, neon, argon, and xenon, for typical laser intensities for each target. The conventional scaling law at fixed range of energy [12–14] can be easily obtained from our universal wave packet. Earlier theoretical

results [12] showed a quite strong contribution from higher-order returns at the single-atom response level. Here we show that under typical experimental conditions, when good phase matching is achieved in the macroscopic medium, only the first return survives.

Following the quantitative rescattering model, we define the wave packet as

$$|W(E)|^2 = S(E)/\sigma(E), \tag{1}$$

where $S(E)$ is the HHG yield and $\sigma(E)$ is the photo-recombination cross section. For each atomic target, the cross section can be exactly calculated numerically within a model potential approach in the single-active electron approximation. The same model potential is used in the TDSE to calculate $S(E)$ [30,32]. In the following we will use a scaled energy $\tilde{E}$ defined as $\tilde{E} = (E - I_p)/U_p$, which corresponds to the returning electron kinetic energy in units of U_p. For photon energy much higher than the ionization potential I_p, quite typical with a mid-IR driving laser pulse, $\tilde{E} \approx E/U_p$.

We use three different methods for analysis: the TDSE, the SFA [33], and the QO theory. To be specific, we now focus on the atomic hydrogen target. A laser pulse of two-cycle flattop envelope with half-cycle turn-on (turn-off) ramps, as shown in Fig. 1(a), with an intensity of 1×10^{14} W/cm^2, and the wavelengths from 0.8 to 3.2 μm is used in the TDSE. For SFA and QO analysis, the wavelength is extended up to 6.4 μm. Longer laser pulses are not needed since we will mostly focus on the first return.

We show in Fig. 1(b) a typical time-frequency trace of the induced dipole acceleration from the TDSE for the wavelength of 2.4 μm. This time-frequency trace is calculated using a wavelet transformation [34,35]. We can clearly identify the first return in the time range $t = [-0.57: -0.07]$ in units of optical cycle (OC) [as indicated by the vertical dashed lines in Fig. 1(b)]. The electron, which recombines during this time interval, was born into the continuum at the ionization time near $t_i \approx -1$ OC. Note that the first return can be further separated into two branches, associating with the long and short trajectories in the QO theory. For our analysis of the TDSE results in the following, we will define "short"(or "long") trajectory contribution to HHG as due to the recombination in the time range $t_r = [-0.57: -0.3]$ OC (or $t_r = [-0.3: -0.07]$ OC). The HHG signal due to the first return is the coherent contribution of short and long trajectories. In the subsequent subcycles, higher-order returns start to show up. Since the HHG spectrum and wave packet typically oscillate on a fine energy scale, we smooth out the fast oscillation by using Bezier interpolation. A typical example of the wave packet and its Bezier curve are shown in Fig. 1(c) for the wavelength of 2.4 μm.
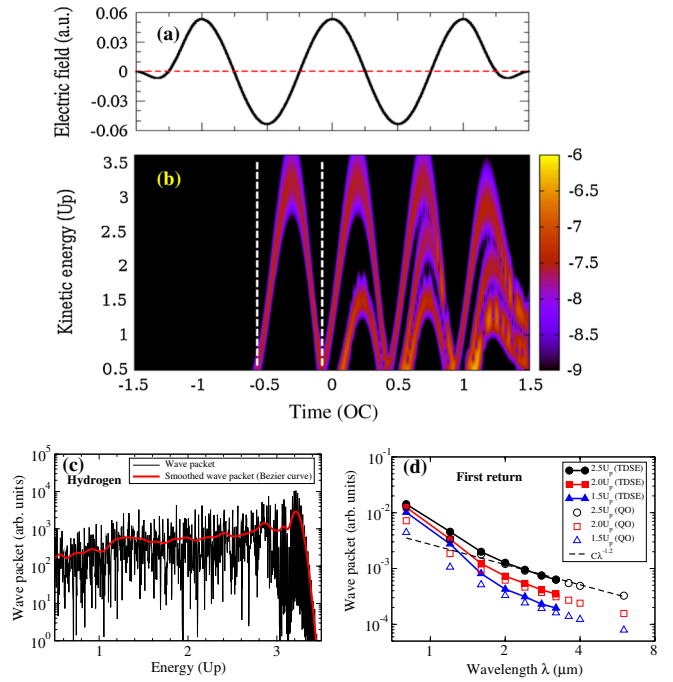

FIG. 1 (color online).   (a) Typical flattop electric field used in our calculation. (b) Typical time-frequency trace of the induced dipole acceleration from TDSE. (c) Typical returning electron wave packet and its Bezier curve. (d) TDSE results for electron wave packet $|W(\tilde{E})|^2$ due to first return at fixed scaled energies of 2.5, 2.0, and 1.5 vs laser wavelength from 0.8 to 3.2 μm. QO results are also shown (symbols), from 0.8 to 6 μm. All results here are for atomic hydrogen with laser intensity of 1×10^{14} W/cm^2.

In Fig. 1(d) we show the wave packets due to the first return at different scaled energies $\tilde{E} = 2.5$, 2.0, and 1.5, as a function of laser wavelength from both TDSE and QO theory. The QO results have been normalized to the TDSE result at 3.2 μm, for $\tilde{E} = 2.5$. It appears that the wave packet scales approximately as $\lambda^{-1.2}$ (dashed line) for both methods at wavelengths above 2.4 μm for all three energies considered. At wavelengths shorter than 2.4 μm, the wave packet drops faster, especially for smaller $\tilde{E}$. This result also indicates that the QO is quite adequate for describing electron wave packet. We note that within the QO the scaling slowly approaches λ^{-1} at even longer wavelengths (above 6 μm) [36]. This result also agrees with the numerical result from the SFA. However, at such long wavelengths, one will need to take into account the magnetic-field effect [37]. Therefore, in this Letter we will limit ourselves only to the wavelengths shorter than about 6 μm, when the scaling is approximately $\lambda^{-1.2}$.

According to the above analysis we now define a *rescaled* wave packet $|\tilde{W}(\tilde{E})|^2 = (\lambda/\lambda_0)^{1.2}|W(\tilde{E})|^2$, where λ_0 is a reference wavelength, introduced for the dimension purpose. The main result of this Letter is presented in Fig. 2(a) where the rescaled wave packets from the first return are shown as a function of $\tilde{E}$ for different wavelengths at a laser intensity of 1×10^{14} W/cm^2. Just above
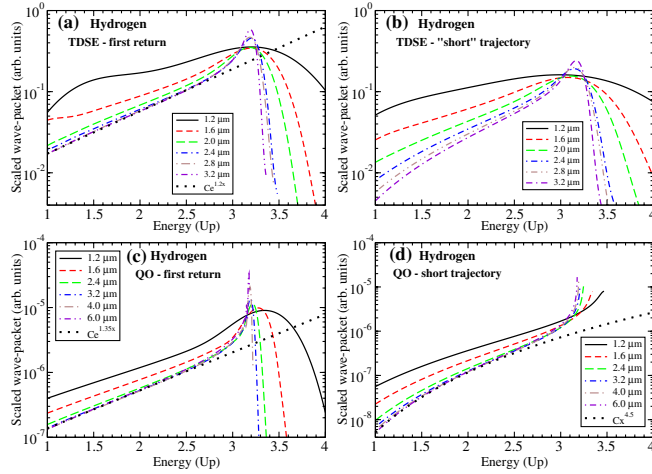
FIG. 2 (color online).   (a) TDSE results for rescaled wave
packets $|\tilde{W}(\tilde{E})|^2$ from atomic hydrogen due to the first return
with different laser wavelengths. The curves have been smoothed
out using Bezier interpolation. (b) Same as (a), but for short
trajectories. (c) and (d) Same as (a) and (b), respectively, but from
QO theory.

0.8 μm, the rescaled wave packet decreases very fast with
increasing wavelength λ. It then decreases slowly with $\lambda >$
2.4 μm and virtually converges to a common shape for
$\tilde{E} \lesssim 3$. This universal shape can be approximated by an
exponential function of the form $e^{1.2\tilde{E}}$ (dotted line). Above
$\tilde{E} \approx 3$ the wave packet still experiences small changes with
increasing λ due to the influence of the abrupt cutoff, which
becomes sharper for longer wavelength [12]. Since the
short trajectory contributes most to the macroscopic HHG
in a typical good phase matching condition, we also show
in Fig. 2(b) the rescaled wave packet from the short
trajectory vs scaled energy. The convergence appears to
be somewhat slower than for the first return. These TDSE
results have been confirmed by our QO calculation shown
in Fig. 2(c) and 2(d) for the first return and short trajectory,
respectively. There are some small differences in the slopes
of the wave packets from the two methods. Similarly to the
TDSE results, we also notice slower convergence of the
short-trajectory wave packet to a universal limit, as com-
pared to the first return.

A nice feature of our approach is that the rescaled wave
packet has a universal behavior in the long wavelength
limit, nearly independent of the target. As shown in
Fig. 3(a), the wave packet due to the first return for
different targets with long wavelengths driving the laser
are indeed virtually identical. Here laser intensities used in
the TDSE calculation are $0.8I_0$, $1I_0$, $1.5I_0$, and $2I_0$ for Xe,
H, Ar, and Ne, respectively, where $I_0 = 10^{14}$ W/cm^2,
while the wavelengths are 3.6, 3.2, 2.8, and 2.4 μm,
respectively. Note that higher laser intensities are used in
the calculations for targets with higher I_p. This intensity
range is also quite typical for an efficient phase matching in
real experiments [11]. Small modifications in laser intensity
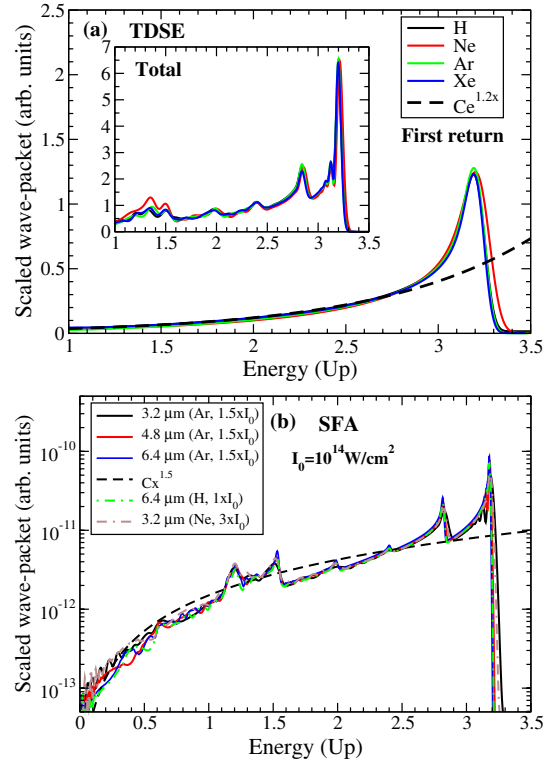

FIG. 3 (color online).   (a) Wave packets due to the first return
from the TDSE for different atoms as shown in the labels. See text
for laser parameters. The same are shown in the inset, but for the
total wave packets. (b) Total rescaled wave packets from the SFA
for different targets. Laser intensities and wavelengths are given
in the labels. In both (a) and (b) the wave packets from different
targets have been normalized to account for the differences in
ionization rates.

do not change our conclusion. Our choice of the shorter
wavelengths used for Ar and Ne is mostly for computa-
tional convenience as computer time for the TDSE
increases drastically with laser wavelength.

The universality of the returning wave packet is not
limited to the first return. Indeed, with still relatively short
wavelengths used in the TDSE, the *total* (from the whole
laser pulse) rescaled wave packets from different targets are
nearly identical; see the inset of Fig. 3(a). We have further
carried out calculations for longer wavelengths within the
SFA. The SFA results shown in Fig. 3(b) for Ar with
different wavelengths confirm the convergence of the total
wave packet for $\lambda \gtrsim 3.2$ μm. Furthermore, the total wave
packets from H and Ne also converge to the same universal
shape. Here, all the SFA calculations were done with the
pulse shape shown in Fig. 1(a). By using the QO theory we
found that not only the first return, but any higher-order
return has its own universal wave packet [36] that leads to
the universal shape for the total wave packet. We note that a
similar study within the SFA on high-order return con-
tributions at the single atom level has been reported
recently by He *et al.* [38].

Overall, the universal total wave packet from a flattop pulse can be approximated by $|\tilde{W}(\tilde{E})|^2 \propto \tilde{E}^{1.5}$ [dashed line in Fig. 3(b)]. Taking into account that $|\tilde{W}(\tilde{E})|^2 \propto \lambda^{1.2}|W(\tilde{E})|^2$, $E \approx \tilde{E}U_p$, and $U_p \propto \lambda^2$, it follows that $|W(E)|^2 \propto \lambda^{-4.2}$ for a fixed E. For a fixed energy E, the photorecombination cross section only gives an overall factor. The scaling law for HHG yield at a fixed energy E should therefore be the same as for the wave packet $|W(E)|^2$. This argument holds approximately for a small range of energy, say, $E = [20–50]$ eV, as used in [12–14]. Their scaling law of $S(E) \propto \lambda^{-(5-6)}$ for HHG yield was somewhat less favorable compared to our result. The difference is mainly due to the fact that earlier analyses [12–14] were limited to wavelengths below 2 μm, where the wave packet drops faster with wavelength [see Fig. 1(d)]. Our scaling law strictly applies only to the long wavelength limit, typically above 3 μm, when the wave packet virtually converges to a universal shape.

We emphasize that the universal total wave packet depends on the actual shape (envelope) of the laser pulse. Furthermore, the universal behavior is expected to break down when depletion of the ground state becomes significant within a half optical cycle.

Macroscopic phase matching of HHG has been known to be quite different for short and long trajectories [39]. However, the effect of macroscopic propagation has not been well documented for higher-order returns from mid-IR pulses. To illustrate this effect, we use the QO theory to separate the different contributions from multiple returns as well as short and long trajectories of the first return. Returns up to the third order are included in our calculation. Our simulations are shown in Fig. 4(a) and 4(b) for a typical gas jet experimental setup with a tightly focused laser beam, for two different gas jet positions at 1 and 3.5 mm after the focus, respectively. The target is Ar and the laser wavelength is 1.6 μm. We keep the laser intensity of 1×10^{14} W/cm^2 at the center of the gas jet. The other parameters are the same for the two cases. As evident from Fig. 4(a), long trajectories dominate for the gas jet near the laser focus. Higher-order returns contribute quite insignificantly to the total macroscopic HHG yields, mainly below about 50 eV. The contribution comes mostly from the second return which has a cutoff near $I_p + 1.5U_p \approx 51$ eV. For a good phase matching case, shown in Fig. 4(b), short trajectories dominate and there is virtually no contribution from higher order returns. This result is not totally surprising since an electron with a higher order return spends a longer amount of time in the continuum, and, therefore, it accumulates a larger phase due to the laser. The variation of laser intensity in the interaction region would wash out a higher order return contribution.

In conclusion, we have shown that a returning electron wave packet in high harmonic generation with mid-IR laser pulses converges to a universal shape at the long wave
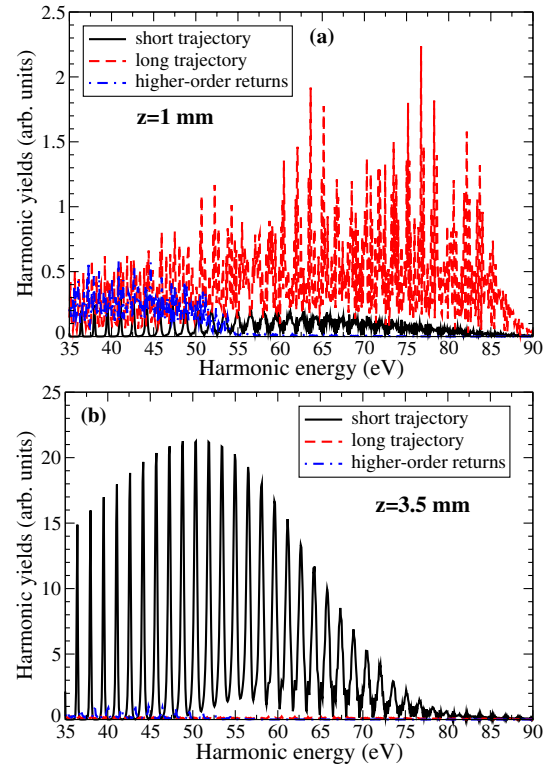

FIG. 4 (color online). Macroscopic HHG yields after propagating in the Ar gas jet of 1 mm thick placed at $z = 1$ mm (a) and $z = 3.5$ mm (b) after the laser focus. Single atom induced dipole is calculated by the QO theory, for a sine-squared envelope laser pulse with 1.6 μm wavelength, 1×10^{14} W/cm^2 peak intensity (at the center of gas jet), and a 30-cycle total duration. The beam waist is 36 μm.

length limit. A nearly universal shape starts to occur for wavelengths as short as about 3 μm for most atomic targets under typical laser intensities of order 1×10^{14} W/cm^2 or so. This indicates that, with regard to the returning electron wave packet, the main physics at long wavelengths is in fact quite simple and can be explained accurately using semiclassical approaches such as the SFA and the QO theory, even though the numerical calculation of the TDSE is much more demanding, as compared to the case of a Ti: sapphire laser. Thus, the knowledge of the universal rescaled wave packet provides a simple and practical method for quick estimates of HHG yield from different targets with midinfrared laser pulses. We have also shown that higher order returns are quite negligible in good phase matching condition for typical experimental setups with tightly focused laser beams.

[1] T. Popmintchev, M. C. Chen, P. Arpin, M. M. Murnane, and H. C. Kapteyn, Nat. Photonics **4**, 822 (2010).

[2] E. Goulielmakis, M. Schultze, M. Hofstetter, V. S. Yakovlev, J. Gagnon, M. Uiberacker, A. L. Aquila, E. M. Gullikson, D. T. Attwood, R. Kienberger, F. Krausz, and U. Kleineberg, Science **320**, 1614 (2008).

[3] K. Zhao, Q. Zhang, M. Chini, Y. Wu, X. Wang, and Z. Chang, Opt. Lett. **37**, 3891 (2012).

[4] R. López-Martens, K. Varjú, P. Johnsson, J. Mauritsson, Y. Mairesse, P. Salières, M. B. Gaarde, K. J. Schafer, A. Persson, S. Svanberg, C. G. Wahlström, and A. L'Huillier, Phys. Rev. Lett. **94**, 033001 (2005).

[5] J. Itatani, J. Levesque, D. Zeidler, H. Niikura, H. Pepen, J. C. Kiefer, P. B. Corkum, and D. M. Villeneuve, Nature (London) **432**, 867 (2004).

[6] M. Lein, J. Phys. B **40**, R135 (2007).

[7] C. D. Lin, A. T. Le, Z. Chen, T. Morishita, and R. R. Lucchese, J. Phys. B **43**, 122001 (2010).

[8] P. Colosima, G. Doumy, C. I. Blaga, J. Wheeler, C. Hauri, F. Catoire, J. Tate, R. Chirla, A. M. March, G. G. Paulus, H. G. Muller, P. Agostini, and L. F. DiMauro, Nat. Phys. **4**, 386 (2008).

[9] K. Hong, S. Huang, J. Moses, X. Fu, C. Lai, G. Cirmi, A. Sell, E. Granados, P. Keathley, and F. Kärtner, Opt. Express **19**, 15538 (2011).

[10] G. Andriukaitis, T. Balciunas, S. Alisauskas, A. Pugzlys, A. Baltuska, T. Popmintchev, M. C. Chen, M. M. Murnane, and H. C. Kapteyn, Opt. Lett. **36**, 2755 (2011).

[11] T. Popmintchev *et al.*, Science **336**, 1287 (2012).

[12] J. Tate, T. Auguste, H. G. Muller, P. Salières, P. Agostini, and L. F. DiMauro, Phys. Rev. Lett. **98**, 013901 (2007).

[13] K. Schiessl, K. L. Ishikawa, E. Persson, and J. Burgdörfer, Phys. Rev. Lett. **99**, 253903 (2007).

[14] M. V. Frolov, N. L. Manakov, and A. F. Starace, Phys. Rev. Lett. **100**, 173001 (2008).

[15] V. Yakovlev, M. Ivanov, and F. Krausz, Opt. Express **15**, 15351 (2007).

[16] E. L. Falcão-Filho, V. M. Gkortsas, A. Gordon, and F. X. Kätner, Opt. Express **17**, 11217 (2009).

[17] J. A. Pérez-Hernández, L. Roso, and L. Plaja, Opt. Express **17**, 9891 (2009).

[18] D. R. Austin and J. Biegert, Phys. Rev. A **86**, 023813 (2012).

[19] T. Auguste, F. Catoire, P. Agostini, L. F. DiMauro, C. C. Chirila, V. S. Yakovlev, and P. Salières, New J. Phys. **14**, 103014 (2012).

[20] B. Shan and Z. Chang, Phys. Rev. A **65**, 011804(R) (2001).

[21] A. D. Shiner, C. Trallero-Herrero, N. Kajumba, H.-C. Bandulet, D. Comtois, F. Légaré, M. Giguère, J-C. Kieffer, P. B. Corkum, and D. M. Villeneuve, Phys. Rev. Lett. **103**, 073902 (2009).

[22] C. Jin, A. T. Le, and C. D. Lin, Phys. Rev. A **83**, 023411 (2011).

[23] P. Salieres, B. Carre, L. Le Deroff, F. Grasbon, G. G. Paulus, H. Walther, R. Kopold, W. Becker, D. B. Milosevic, A. Sanpera, and M. Lewenstein, Science **292**, 902 (2001).

[24] D. B. Milosevic and W. Becker, Phys. Rev. A **66**, 063417 (2002).

[25] G. Sansone, C. Vozzi, S. Stagira, and M. Nisoli, Phys. Rev. A **70**, 013411 (2004).

[26] H. R. Reiss, Phys. Rev. A **82**, 023418 (2010).

[27] O. I. Tolstikhin and T. Morishita, Phys. Rev. A **86**, 043417 (2012).

[28] T. Morishita, A. T. Le, Z. Chen, and C. D. Lin, Phys. Rev. Lett. **100**, 013903 (2008).

[29] A. T. Le, R. R. Lucchese, M. T. Lee, and C. D. Lin, Phys. Rev. Lett. **102**, 203001 (2009).

[30] A. T. Le, R. R. Lucchese, S. Tonzani, T. Morishita, and C. D. Lin, Phys. Rev. A **80**, 013401 (2009).

[31] M. V. Frolov, N. L. Manakov, T. S. Sarantseva, M. Yu. Emelin, M. Yu. Ryabikin, and A. F. Starace, Phys. Rev. Lett. **102**, 243901 (2009).

[32] T. Morishita, Z. Chen, S. Watanabe, and C. D. Lin, Phys. Rev. A **75**, 023407 (2007).

[33] M. Lewenstein, Ph. Balcou, M. Yu. Ivanov, A. L'Huillier, and P. B. Corkum, Phys. Rev. A **49**, 2117 (1994).

[34] X. M. Tong and S.-I. Chu, Phys. Rev. A **61**, 021802(R) (2000).

[35] P. Antoine, B. Piraux, and A. Maquet, Phys. Rev. A **51**, R1750 (1995).

[36] A. T. Le, H. Wei, C. Jin, and C. D. Lin (to be published).

[37] C. Hernandez-Garcia, J. A. Perez-Hernandez, T. Popmintchev, M. M. Murnane, H. C. Kapteyn, A. Jaron-Becker, A. Becker, and L. Plaja, Phys. Rev. Lett. **111**, 033002 (2013).

[38] L. He, Y. Li, Z. Wang, Q. Zhang, P. Lan, and P. Lu, Phys. Rev. A **89**, 053417 (2014).

[39] M. B. Gaarde, J. L. Tate, and K. J. Schafer, J. Phys. B **41**, 132001 (2008).